QUANTUM AND GRAVITATIONAL PHYSICS
3:018, 23 p., 14.02.2022; doi:10.9751/QGPH.3-018.7715
ISSN 2181-0486; EISSN 2181-0508

Effects of gravity around charged and rotating collapsars in metrics with independent parameters

Zahid Zakir[1]

Abstract

The Kerr-Newman metric around charged and rotating sources, as well as Reissner-Nordström and Kerr, included the total mass at infinity, depending on the charge and rotation parameter, and therefore, as solution up to an unknown function of independent parameters, it was only an intermediate stage in solving the problem. The complete solution as a metric with independent parameters was recently given by the author (Zakir, 2022). For a ball with a charge on the surface, the new metrics includes three independent parameters - surface radius, charge, and ball's gravitational radius, equal to the gravitational radius of neutral matter. The electric field energy exists only outside the ball and contributes to the metric with the same sign as the matter. Therefore, the increase in charge enhances gravity and its effects (time dilation and redshifts, orbit radii and shadows). At collapse of the ball, its surface asymptotically approaches the gravitational radius and the ball freezes (in center's rest frame), becoming a frozar. Two parameters remain in its metric and the observable consequences are the same as for a ball with a given surface. The metric around frozar with angular momentum is given by a new form of the Kerr metric including two independent parameters - the gravitational radius at the pole and rotation parameter. In it, the contributions to the metric of the energies of matter and rotation have the same sign, and therefore an increase in rotation parameter enhances gravity and its effects. When there is also a charge on the surface, the metric is given by a new form of the Kerr-Newman metric, also including the gravitational radius at the pole as an independent parameter. Its consequences are a combination of the two previous cases. All these consequences are physically correct, but they are opposite to the conclusions from the standard metrics of Reissner-Nordström, Kerr and Kerr-Newman. In these standard metrics, the dependence of the total mass on the charge and rotation parameter was ignored, which led to erroneous predictions about the weakening of effects of gravity at increasing of these parameters. The present article provides a brief review of the new metrics and a more detailed description of their consequences for observable effects.

Keywords: charged ball, gravitational radius, Reissner-Nordström metric, Kerr metric, Kerr-Newman metric, black hole, frozar, gravity effects, shadow

Content

1.INTRODUCTION 2
2.GRAVITATIONAL FIELDS OF SOURCES WITH A CHARGE ON THE SURFACE 3
  2.1. Metrics with independent parameters for a ball and frozar 3
  2.2. Time dilation and redshifts 5
  2.3. Radii of orbits of photons and massive particles 6
  2.4. The shadow of charged compact sources 8
3.FROZAR WITH ANGULAR MOMENTUM 8
  3.1. A new form of the Kerr metric as a metric with independent parameters 8
  3.2. Proper time dilation and redshifts 11
  3.3. Radii of orbits of photons and massive particles 13
  3.4. The shadow of a rotating collapsar 15
4.COLLAPSAR WITH ANGULAR MOMENTUM AND CHARGE ON THE SURFACE 17
  4.1. Modified Kerr-Newman metric with independent parameters 17
  4.2. Proper time dilation and redshifts 19
5.CONCLUSION 21
  Appendix. The shadow of a rotating collapsar 22
  References 23

[1] *Center for Theoretical Physics and Astrophysics, Tashkent Uzbekistan*, zzakir@qgph.uz ORCID

1. Introduction

In the previous two articles [1,2], it was found a new form of exact solutions of the Einstein equations for the metric around charged and rotating sources with true dependencies on the charge Q and rotation parameter a. It turned out that they differ significantly from the previous dependences contained in the standard metrics, Reissner-Nordström (RN) [3-5] and Kerr [6,7] in particular cases, and Kerr-Newman metrics (KN) [8] in general case (see [9]).

The reason for this discrepancy was that the new metrics are solutions in terms of independent parameters, while the previous metrics were solutions up to an unknown function of these parameters and therefore were only intermediate steps in solving the problem.

Indeed, the former metrics included, as the main integration constant, the total mass of the source at infinity $\bar{M}$, determined from the Schwarzschild solution in the asymptotics. But $\bar{M}$ included, in addition to the mass of the neutral non-rotating matter M, also the mass-equivalent of energies of rotation and electric field. Therefore, $\bar{M}$, be independent of coordinates, was depended on a and Q, i.e., was some function of other parameters of the metric $\bar{M} = f(M,Q,a)$. Since in the general case it is not known how $\bar{M}$ changes when a and Q change, it is also impossible to predict the dependence of the effects of gravity on a and Q.

In fact the dependence $\bar{M}(M,Q,a)$ is different in different models of the structure of the source and, therefore, it can be determined only in a specific physical model of the source. Almost all previous studies of the dependence on a and Q of the properties of collapsars and the effects of gravity proceeded from the arbitrarily taken assumptions that the sources are black holes (BHs) and for them $\bar{M}$ *does not depend* on other parameters of the metric. It is clear that these studies were erroneous already due to the last assumption about the constancy of $\bar{M}$.

For these reasons, in order to complete solution of the problem and eliminate such errors, it is necessary to determine: a) a simplest and realistic model of the source, b) an independent parameter replacing $\bar{M}$ in the metrics, then c) find a function $\bar{M}(M,Q,a)$ in terms of these independent parameters, and finally, d) substituting this dependence into standard metrics with $\bar{M}$, find *the metrics with independent parameters*. Only this form of the metric allows one to correctly study the dependence of the effects of gravity on the parameters of the metric.

All this was done in [1,2], where it was first shown that the simplest realistic model is a dust star with a surface charge, where the independent parameter is the mass of a neutral non-rotating matter M, and then an explicit expression for $\bar{M}(M,Q,a)$ was found. When such a star collapses, its surface freezes (in the center's rest frame) almost at the gravitational radius and the star becomes a frozar (frozen star), for which:

$$\bar{M}(M,Q,a) = M + \frac{a^2 + Q^2}{4MG^2/c^4}, \tag{1}$$

where G is the gravitational constant. Substitution (1) into the standard KN metric with $\bar{M}$ then led to the metric with independent parameters. This form of metric, correct from a physical and consistent from a mathematical points of view, revised both the physical picture and the observable consequences of the KN metric and its special cases, the RN and Kerr metrics.

In the present article a brief review of this new approach and its consequences, studied in [1,2], are presented with new plots of the dependence on a and Q of the gravitational time dilation, redshifts, orbital radii, and the shadow of collapsars. A more detailed description of the consequences of the new approach will be presented in the book [10].

Notice that the internal structure of the collapsar affects to the external effects through the angular momentum and charge distribution. The article takes into account the fact that the real stars can have the charge on the surface only, and at the collapse the surface asymptotically freezes above the gravitational radius on the hypersurfaces of simultaneity $t = const$, where all the effects are described. This picture lies on the basis of the frozar theory, where the surface, as well as the charge, is practically on the gravitational radius. The BH theory is based on the picture of a point source, where the electric field energy and the centrifugal energy diverge, and therefore in this model the mass was implicitly renormalized, as a result of which the dependence of the total mass on other parameters of the metric was lost.

In Sections 2–3 of the article metrics with independent parameters and their consequences are presented, at first for charged and then for rotating frozars, and in Section 4 for the general case when there are both the charge and the angular momentum.

2. Gravitational fields of sources with a charge on the surface

2.1. Metrics with independent parameters for a ball and frozar

The space-time interval outside a charged dust ball in the rest frame of its center can be reduced to the diagonal form:

$$ds^2 = g_{00}(r)c^2dt^2 + g_{11}(r)dr^2 - r^2d\Omega^2, \tag{2}$$

where $d\Omega^2 = d\theta^2 + \sin^2\theta d\varphi^2$. The world time t marks simultaneous events and the ball as an extended object is given on the hypersurfaces of simultaneity $t = const$.

A ball with a charge Q (associated with the ordinary charge e as $Q = e\sqrt{G}/c^2$, unlike a neutral ball, is not a compact source of gravity. Inside its surface with a radius r_b there is only a part of its energy related to the matter and the electric field of the charge inside the ball. The mass-equivalent of this energy gives the ball's mass $M_b(Q)$. The total mass $\bar{M}(r,Q)$ in the sphere of radius $r > r_b$ includes also the mass-equivalent of the energy of the outer electric field in the interval (r_b, r), and this part of the total mass depends on both r and Q.

The external metric for a ball with a charge distributed over the entire volume of the ball was found in 1960 by W. Bonnor [11] and P. Florides [12], who found a contribution to the total mass of the ball at infinity of electric energy outside the ball as: $\Delta\bar{M}(\infty,Q) = e^2/2r_bc^2$, which gives $\bar{M}(\infty,Q) = M_b(Q) + e^2/2r_bc^2$, showing that an increase in Q enhances the gravity (see also [13]). But $M_b(Q)$ was depended on Q because of the internal electric field and this weakness did not allow them to find a metric with independent parameters.

In fact, any real charged ball has the charge on its surface only, where electrostatic equilibrium is reached. For this reason, in [1], the outer metric was obtained for such a realistic case of a ball with *a surface charge* only (Fig. 1), when the ball's mass M *does not depend* on Q. Further, we obtain this metric in a simpler way and study its consequences.

The electric field energy *outside* the sphere of radius r does not contribute to the metric on this sphere, while the electric field energy *inside* this sphere increases the total mass inside this sphere $\bar{M}(r,Q)$. Therefore, the solution of the Einstein-Maxwell equations outside the ball with a charge on the surface (Fig. 1) is easier to obtain directly from the Schwarzschild solution with this effective gravitating mass $\bar{M}(r,Q)$:

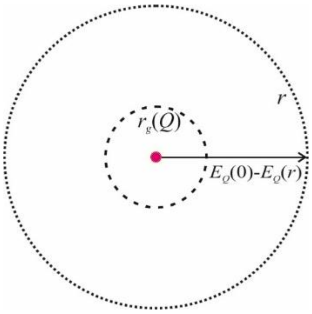

Fig. 1a. Gravitational and electric fields of BHs. A point charge with $r_b \to 0$.

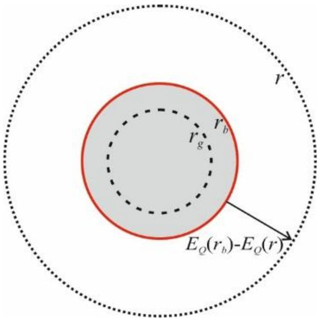

Fig. 1b. Gravitational and electric fields of the ball. A surface charge at $r_b > r_g$.

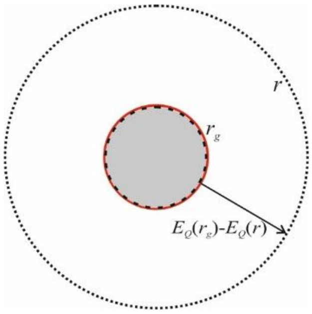

Fig. 1c. Gravitational and electric fields of frozar. A surface charge at $r_b \simeq r_g$.

$$g_{00}(r) = -g_{11}^{-1}(r) = 1 - \frac{r_{gQ}(r)}{r}, \tag{3}$$

where $r_{gQ}(r) = 2G\bar{M}(r,Q)/c^2$ is the effective gravitational radius. Here

$$\bar{M}(r,Q) = M + M_Q(r,r_b). \tag{4}$$

where $M_Q(r,r_b)$ is the mass-equivalent of electric field energy in the interval (r_b, r) [11,12]:

$$M_Q(r,r_b) = \frac{e^2}{2c^2}\left(\frac{1}{r_b} - \frac{1}{r}\right). \tag{5}$$

Substituting (5) into (4) and then substituting the result for $\bar{M}$ into (3), we arrive at a metric with three independent parameters r_b, r_g and Q for a ball with the charge on the surface [1]:

$$g_{00}(r) = -g_{11}^{-1}(r) = 1 - \frac{r_g}{r} - \frac{Q^2}{r}\left(\frac{1}{r_b} - \frac{1}{r}\right) = 1 - \frac{r_g}{r} - \frac{Q^2}{r_b r}\left(1 - \frac{r_b}{r}\right), \quad r \ge r_b, \tag{6}$$

where $r_b > r_g$ and $r_g = 2GM/c^2$ is the gravitational radius of the neutral matter of the ball. Notice, that the outer electric field energy does not affect the metric inside the ball.

In the region $r \ge r_b > r_g$, the metric (6) has no singularities, the expression in parentheses in (6) is positive-definite, the contribution of the electric field energy to the metric grows as Q^2 and has the same sign as the energy of matter. Therefore, growth of Q enhances gravity in $r > r_b$ due to the growth of the electric field energy in the sphere r. This means that the observable effects of gravity (the radii of orbits and shadow, redshifts) in the field of a charged ball increase with growth of Q, and corresponding plots are presented in Section 2.2.

The metric outside the charged collapsar (frozar) in (2) follows from the ball's metric (6) in the asymptotic approaching $r_b \to r_g$ (Fig. 2):

$$g_{00}(r) = -g_{11}^{-1}(r) \simeq \left(1 - \frac{r_g}{r}\right)\left(1 - \frac{Q^2}{r_g r}\right) = 1 - \frac{r_g + Q^2/r_g}{r} + \frac{Q^2}{r^2}, \quad r > r_g. \tag{7}$$

This metric now contains only *two* independent parameters r_g, Q. Denoting

$$r_{gQ}=r_g+\frac{Q^2}{r_g}, \tag{8}$$

metric (7) can be written in the form of a standard RN metric:

$$g_{00}(r)=-g_{11}^{-1}(r)=1-\frac{r_{gQ}}{r}+\frac{Q^2}{r^2}. \tag{9}$$

The RN metric (9) at first, by analogy with the Newtonian theory, was formally considered as a solution for a *point* source [3-6]. In BH theory, this Newtonian picture was directly extrapolated into general relativity (see [9]). Since the physical consequences of the RN metric (9) depend on the choice of dependence r_{gQ} on Q, then the choice of a point source with $r_b \to 0$ [3-6] leads to a divergent electric field energy in (5). As a result, the total mass also became divergent $\bar{M}(Q)\to\infty$ and, therefore, a hidden *mass renormalization* was done, replacing $\bar{M}(Q)$ with the finite "observable" mass $\bar{M}_{obs}$. In this case, the dependence of $\bar{M}_{obs}$ on Q was lost and $\bar{M}_{obs}$ was considered independent on Q (even after this dependence had already been found in [11-13]).

Such neglecting of the dependence one of the parameters on others in the standard RN metric led to erroneous consequences in BH theory, such as a complicated structure of spacetime with two horizons and predictions that the growth of Q weakens gravity, reducing the effects of gravity (time dilation, redshifts, the radii of orbits and shadow) [9,14].

2.2. Time dilation and redshifts

For a test particle resting near a charged source at the point $(r,\theta,\varphi)=const$, the proper time interval between two events $\Delta\tau=g_{00}^{1/2}(r)\Delta t$ is less than the world time interval Δt between the same events. This is the gravitational dilation of proper times. For the metrics for the ball (6), frozar (7) and BH (9) we have, correspondingly:

$$\Delta\tau_{ball}=\Delta t\left[1-\frac{r_g}{r}-\frac{Q^2}{r_b r}\left(1-\frac{r_b}{r}\right)\right]^{1/2}, \tag{10}$$

$$\Delta\tau_{froz}\simeq\Delta t\left(1-\frac{r_g}{r}\right)^{1/2}\left(1-\frac{Q^2}{r_g r}\right)^{1/2}, \tag{11}$$

$$\Delta\tau_{BH}=\Delta t\left(1-\frac{r_{gQ}}{r}+\frac{Q^2}{r^2}\right)^{1/2}. \tag{12}$$

Notice that in BH theory, the normalization condition $r_{gQ}=r_g$ at $Q=0$ was supplemented with the assumption that r_{gQ} is independent of Q at $Q\neq 0$ also [9,14].

In the case of a ball and frozar (10)-(11), the growth of Q reduces the factor $g_{00}^{1/2}(r)$, which means that it increases gravity and, as the result, the dilation of proper times becomes stronger. Plots for the case $r=3r_g$ are shown in Fig. 3, where it can be seen that in the case of frozar, the time dilation is similar to the case of a ball, but stronger. Frozar is the same ball, but its surface radius $r_b\simeq r_g$ is the smallest among balls of the same mass, and therefore the total electric field energy $Q^2/2r_b$, inversely proportional r_b, is the largest, as its contribution to the metric. In the BH theory, the growth of Q under the condition $r_{gQ} = const$ increases $g_{00}^{1/2}(r)$ in (12), by weakening gravity and its effects, in particular, it weakens the time dilation.

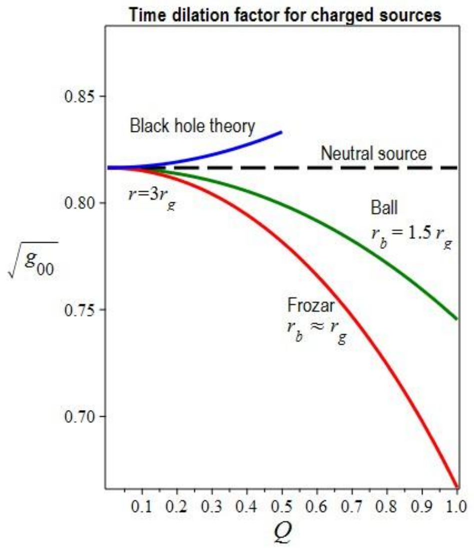

Fig. 3. Charge dependence of the time dilation factor $g_{00}^{1/2}(r)$ at $r = 3r_g$ for a ball with $r_b = 1.5r_g$ (10), a frozar with $r_b \simeq r_g$ (11) and a BH (12).

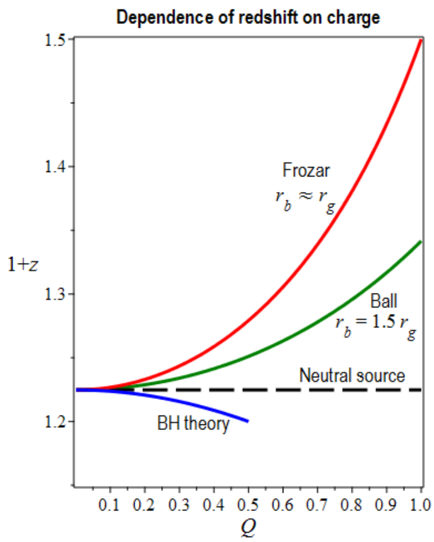

Fig. 4. Dependence of redshift $1+z = g_{00}^{-1/2}(r)$ on charge at $r = 3r_g$ for a ball (13), a frozar (14) and a BH (15).

The gravitational redshift follows from the gravitational dilation of proper times. The frequency ω (in terms t) of photons, emitted by a source resting at the point (r,θ,φ) near the ball or frozar, at receiving by a distant observer, will less than the frequency ω_0 of local photons emitted near the observer: $\omega < \omega_0$. The redshift factor $1+z = \omega_0/\omega = g_{00}^{-1/2}(r)$ for the ball, frozar and BH is given by the expressions (Fig. 4):

$$1+z_{ball} = \left[1 - \frac{r_g}{r} - \frac{Q^2}{r_b r}\left(1 - \frac{r_b}{r}\right)\right]^{-1/2}, \quad (13)$$

$$1+z_{froz} = \frac{\omega_0}{\omega} = \left(1 - \frac{r_g}{r}\right)^{-1/2}\left(1 - \frac{Q^2}{r_g r}\right)^{-1/2}, \quad (14)$$

$$1+z_{BH} = \frac{\omega_0}{\omega} = \left(1 - \frac{r_{gQ}}{r} + \frac{Q^2}{r^2}\right)^{-1/2}. \quad (15)$$

The fact that the BH theory predicts the charge dependences of time dilation and redshifts opposite to the case of an ordinary ball shows the unphysical nature of these predictions. At the same time, the predictions of the frozar theory are the same as for a ball, but the electric field energy is greater due to the smaller radius of the surface and the gravity effects are stronger.

2.3. Radii of orbits of photons and massive particles

The equations of motion in a static gravitational field with a metric of the form (9) and their solutions for geodesic trajectories, in particular, for several distinguished orbits, expressed in terms of r_{gQ}, are well known (see [9,14]). The results for the metric with independent

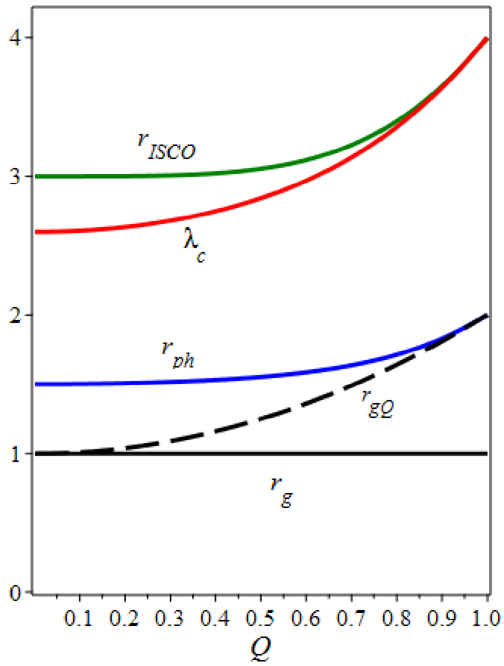

Fig. 5. Radii of orbits and shadow around a frozar.

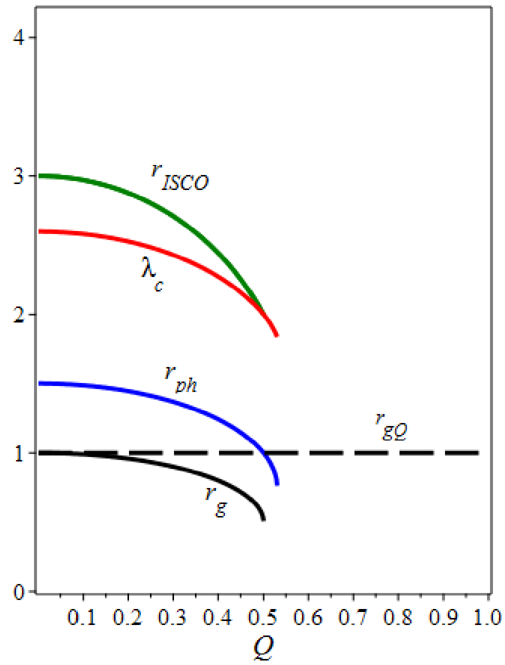

Fig. 6. Radii of orbits and shadow in the BH theory.

parameters (7) follow from them when r_{gQ} is replaced by r_g according (8). Therefore, we present only the results for the dependence of the gravity effects on Q.

The formulas for the radii of the photon orbit r_{ph} and the innermost stable circular orbit of a massive particle r_{ISCO}, expressed in terms of r_{gQ} (see [9,14]), after taking into account the dependence $r_{gQ} = r_g + Q^2 / r_g$, take the form:

$$r_{ph} = \frac{3}{4}\left(r_g + \frac{Q^2}{r_g}\right)\left(1 + \sqrt{1 - \frac{32Q^2}{9(r_g + Q^2/r_g)^2}}\right), \tag{16}$$

$$r_{ISCO} = \frac{1}{2}\left(r_g + \frac{Q^2}{r_g}\right)\left[2 + \xi + \frac{1}{\xi}\left(4 - \frac{12Q^2}{(r_g + Q^2/r_g)^2}\right)\right], \tag{17}$$

$$\xi = 4\left[2 + \frac{8Q^4}{r_{gQ}^4} - \frac{Q^2}{r_{gQ}^2}\left(9 - \sqrt{\left(1 - \frac{2Q}{r_{gQ}}\right)\left(5 - \frac{8Q}{r_{gQ}}\right)}\right)\right]^{1/3}.$$

The gravitational radius of a frozar practically does not depend on $|Q|$, i.e. $r_g = const$, and it follows from the expressions (16)-(19) that the radii r_{ph} and r_{ISCO} grow almost as Q^2. The corresponding plots built according to ((16)-(19) are shown in Figs. 5-6.

2.4. The shadow of charged compact sources

The radius of the shadow of a charged frozar λ_c is given by the expression [9]:

$$\lambda_c = \frac{r_{ph}}{\sqrt{g_{00}(r_{ph})}}. \tag{18}$$

Substituting g_{00} from (7) and r_{ph} from (16), we obtain the shadow radius formula expressed in terms of the independent parameters:

$$\lambda_c = \frac{3}{4}\left(r_g + \frac{Q^2}{r_g}\right)\cdot\frac{1+\sqrt{1-32Q^2/9(r_g+Q^2/r_g)^2}}{\sqrt{(1-r_g/r_{ph})(1-Q^2/r_g r_{ph})}}. \tag{19}$$

Thus, λ_c grows almost as Q^2 and the pictures of this dependence are shown in Fig. 5. The pictures of the previous prediction of the BH theory, presented in Fig. 6, show an inverse relationship, that the radius of the shadow allegedly decreases with increasing the charge. A more visual picture of the shadow is shown in Fig. 7.

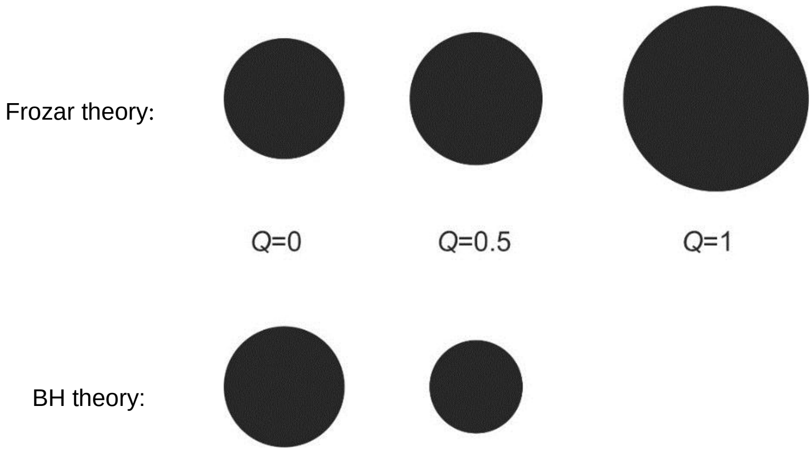

Fig. 7. Dependence of the shadow on the charge for frozars (top) and BHs (bottom).

3. Frozar with angular momentum

3.1. A new form of the Kerr metric as a metric with independent parameters

For a rotating source with a mass of matter M and angular momentum $J = Mac$, where the rotation parameter $a = J / Mc$ is the angular momentum per unit mass (divided by the speed of light c), the line element around it takes the form:

$$ds^2 = g_{00}c^2dt^2 + g_{11}dr^2 + g_{22}d\theta^2 + g_{33}d\varphi^2 + 2g_{03}cdtd\varphi, \tag{20}$$

where t - world time and the metric depend only on r and θ. At using the notations

$$\rho^2(\theta) = r^2 + a^2\cos^2\theta, \quad \Delta = r^2 - r_{gE}(a)r + a^2, \tag{21}$$

the standard Kerr metric [6] in the Boyer-Lindquist coordinates [7] takes the form:

$$ds^2 = \left(1 - \frac{r_{gE} r}{\rho^2}\right) c^2 dt^2 - \frac{\rho^2}{\Delta} dr^2 - \rho^2 d\theta^2 -$$
$$- \left(r^2 + a^2 + \frac{r_{gE} r a^2}{\rho^2} \sin^2\theta\right) \sin^2\theta \, d\varphi^2 + \frac{2 r_{gE} r a c}{\rho^2} \sin^2\theta \, d\varphi dt, \tag{22}$$

Here $r_{gE}(a)$ is the gravitational radius at the equator, defined by the condition (Fig. 8):

$$g_{00}(r_{gE}, \pi/2) = 0. \tag{23}$$

At $a \to 0$, it becomes equal to the gravitational radius at the pole: $r_{gE}(0) = r_{gP}$, which no longer depends on the rotation parameter a.

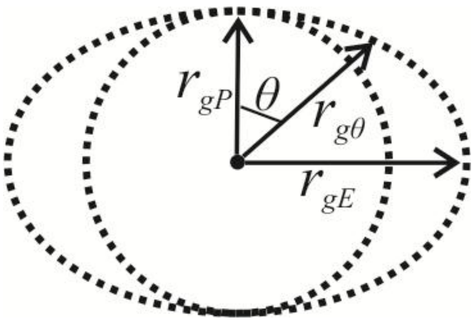

Fig. 8a. Structure of BH with angular momentum.

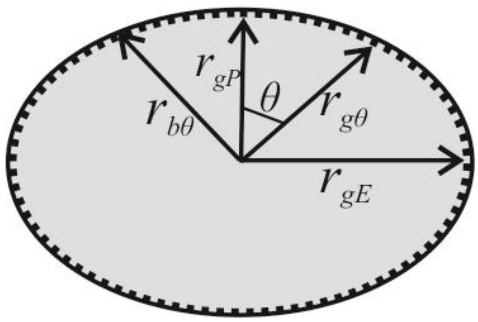

Fig. 8b. Structure of frozar with angular momentum and the radius-vector of the surface $\mathbf{r}_{b\theta}$.

On the equatorial plane ($\theta = \pi/2$, $\rho^2 = r^2$) (22) is simplified and takes the form:

$$ds^2 = \left(1 - \frac{r_{gE}}{r}\right) c^2 dt^2 - \frac{r^2}{\Delta} dr^2 - \left(r^2 + a^2 + \frac{r_{gE} a^2}{r}\right) d\varphi^2 + \frac{2 r_{gE} a c}{r} d\varphi dt, \tag{24}$$

where the condition (23), defining the physical meaning of r_{gE}, is satisfied. At the pole ($\theta = 0$ and $\rho^2(0) = r^2 + a^2$) (22) takes a simple form:

$$ds^2 = \frac{\Delta}{r^2 + a^2} c^2 dt^2 - \frac{r^2 + a^2}{\Delta} dr^2. \tag{25}$$

The gravitational radius at the pole r_{gP} is defined by the condition:

$$g_{00}(r_{gP}, 0) = \frac{\Delta_P}{r^2 + a^2} = 0, \quad \Delta_P \equiv r_{gP}^2 - r_{gE} r_{gP} + a^2 = 0. \tag{26}$$

Dividing the last equality by r_{gP}, we can express r_{gE} in terms of r_{gP}:

$$r_{gE} = r_{gP} + \frac{a^2}{r_{gP}}. \tag{27}$$

As shows (27), r_{gE}, in addition to r_{gP}, also includes the contribution of the rotational energy proportional to a^2, because of which r_{gE} grows as a^2. The modification of the Kerr metric (22), therefore, is reduced to the replacement of the dependent parameter $r_{gE}(a)$ by the independent one r_{gP} using (27). At first, we express Δ in (21) through r_{gP} as:

$$\Delta = r^2 - \left(r_{gP} + \frac{a^2}{r_{gP}}\right) r + a^2 = r^2\left(1 - \frac{r_{gP}}{r}\right)\left(1 - \frac{a^2}{r_{gP} r}\right), \tag{28}$$

and, by inserting into (25), we obtain a line element at the pole with independent parameters:

$$ds^2 = \frac{r^2}{\bar{\rho}^2}\left(1 - \frac{r_{gP}}{r}\right)\left(1 - \frac{a^2}{r_{gP} r}\right) c^2 dt^2 - \frac{\bar{\rho}^2}{r^2}\left(1 - \frac{r_{gP}}{r}\right)^{-1}\left(1 - \frac{a^2}{r_{gP} r}\right)^{-1} dr^2. \tag{29}$$

Here $\bar{\rho}^2 = r^2 + a^2$ and the role of r_{gP} as the gravitational radius is clear. Substituting (24) into (27) then gives a line element at the equator with independent parameters:

$$\begin{aligned} ds^2 = {} & \left(1 - \frac{r_{gP}}{r} - \frac{a^2}{r_{gP} r}\right) c^2 dt^2 - \left(1 - \frac{r_{gP}}{r}\right)^{-1}\left(1 - \frac{a^2}{r_{gP} r}\right)^{-1} dr^2 - \\ & - \left(r^2 + a^2 + \frac{a^2 r_{gP}}{r} + \frac{a^4}{r_{gP} r}\right) d\varphi^2 + \frac{2ac}{r}\left(r_{gP} + \frac{a^2}{r_{gP}}\right) d\varphi dt, \end{aligned} \tag{30}$$

Thus, the weakness of the standard form of the Kerr metric (22) is the fact that one of the two parameters included in it, r_{gE}, depends on the second, a, in the form (27). To correct this weakness, as it was shown for the metrics at the pole and the equator, in the general Kerr metric (22) it is necessary to express r_{gE} through r_{gP} according to (27), which gives:

$$\begin{aligned} ds^2 = {} & \frac{r^2}{\rho^2}\left[1 - \frac{r_{gP}}{r} - \frac{a^2}{r_{gP} r}\left(1 - \frac{r_{gP}}{r}\cos^2\theta\right)\right] c^2 dt^2 - \frac{\rho^2}{\Delta} dr^2 - \rho^2 d\theta^2 - \\ & - \left[r^2 + a^2 + \frac{ra^2}{\rho^2}\left(r_{gP} + \frac{a^2}{r_{gP}}\right)\sin^2\theta\right]\sin^2\theta\, d\varphi^2 + \frac{2rac}{\rho^2}\left(r_{gP} + \frac{a^2}{r_{gP}}\right)\sin^2\theta\, d\varphi dt \end{aligned} \tag{31}$$

with Δ from (28). This is the Kerr metric with two independent parameters r_{gP} and a.

The gravitational radius in the general case $r_{g\theta}$, at which $g_{00}(r,\theta)$ vanishes, is expressed in terms of independent parameters r_{gP} and a as:

$$r_{g\theta} = \frac{1}{2}\left(r_{gP} + \frac{a^2}{r_{gP}}\right) + \sqrt{\frac{1}{4}\left(r_{gP} + \frac{a^2}{r_{gP}}\right)^2 - a^2\cos^2\theta}. \tag{32}$$

At the pole, this gives r_{gP}, at the equator r_{gE}, and in general $r_{g\theta}$ describes an oblate spheroid (Fig. 7), to which the surface of a rotating source asymptotically tends at collapse $r_{b\theta} \to r_{g\theta}$.

At $r > r_{g\theta}$, the metric (31) has no singularities, and it is clearly seen that an increase in a reduces g_{00}, and therefore *enhances* the gravity due to the contribution of the rotational energy. As a result, gravity effects, such as redshifts, average radii of orbits and shadow, in the field of a rotating source *increase* with increasing a. The corresponding formulas and plots are presented in Sections 3.2 - 3.4.

However, in the BH theory, at studying the dependence of the observable effects on a the parameter $r_{gE}(a)$ was assumed to be constant $r_{gE} = const$, and this led to erroneous consequences that the growth of a, i.e. adding a positive rotational energy, *weakens* the gravity of the source and therefore reduces the observable effects of gravity [9,15].

3.2. Proper time dilation and redshifts

In the presence of angular momentum, gravitational time dilation, i.e. deceleration of the proper time τ with respect to t at the point $(r,\theta,\varphi) = const$, is described by the decreasing of the interval $\Delta\tau = \Delta t\, g_{00}^{1/2}(r,\theta)$ between two events at this point. According (31) for frozar and (22) for BH, we have:

$$\Delta\tau_{froz} \simeq \Delta t \frac{r^2}{\rho^2}\left[1 - \frac{r_{gP}}{r} - \frac{a^2}{r_{gP} r}\left(1 - \frac{r_{gP}}{r}\cos^2\theta\right)\right]^{1/2}, \tag{33}$$

$$\Delta\tau_{BH} \simeq \Delta t\left(1 - \frac{r_{gE} r}{\rho^2}\right)^{1/2}. \tag{34}$$

Formula (34) follows from the standard RN metric used in black hole theory, assuming that r_{gE} is equal to r_{gP} at $a = 0$ and independent on a also at $a \neq 0$ [9,12].

At the equator ($\theta = \pi/2$) we have, respectively:

$$\Delta\tau_{froz} \simeq \Delta t\left(1 - \frac{r_{gP}}{r} - \frac{a^2}{r_{gP} r}\right)^{1/2}, \tag{35}$$

$$\Delta\tau_{BH} \simeq \Delta t\left(1 - \frac{r_{gE}}{r}\right)^{1/2}, \tag{36}$$

and on the pole ($\theta = 0$):

$$\Delta\tau_{froz} \simeq \Delta t\left(\frac{(1 - r_{gP}/r)(1 - a^2/r_{gP} r)}{1 + a^2/r^2}\right)^{1/2}, \tag{37}$$

$$\Delta\tau_{BH} \simeq \Delta t\left(1 - \frac{r_{gE} r}{r^2 + a^2}\right)^{1/2}. \tag{38}$$

The plots of the dependence on a of the time dilation factor $g_{00}^{1/2}(r,\theta)$ are shown in Fig. 9.

The frequency ω of photons (in terms of t) emitted at point (r,θ,φ) near the collapsar and received by a distant observer is compared with the frequency ω_0 of local photons (emitted near the observer), which gives $\omega < \omega_0$. The redshift factors $1 + z = \omega_0/\omega$ in the cases of the frozar and BH theories are given by the expressions, respectively:

$$1+z_{froz}=\frac{r^2}{\rho^2}\left[1-\frac{r_{gP}}{r}-\frac{a^2}{r_{gP}r}\left(1-\frac{r_{gP}}{r}\cos^2\theta\right)\right]^{-1/2}, \qquad (39)$$

$$1+z_{BH}=\left(1-\frac{r_{gE}r}{\rho^2}\right)^{-1/2}. \qquad (40)$$

For a frozar, the Eq. (39) takes the form at the equator and at the pole, respectively:

$$1+z_{froz}=\left(1-\frac{r_{gP}}{r}-\frac{a^2}{r_{gP}r}\right)^{-1/2}, \qquad (41)$$

$$1+z_{froz}=\left(\frac{1+a^2/r^2}{(1-r_{gP}/r)(1-a^2/r_{gP}r)}\right)^{1/2}, \qquad (42)$$

and for BH from (40) the expressions on the equator and pole are, respectively:

$$1+z_{BH}=\left(1-\frac{r_{gE}}{r}\right)^{-1/2}, \quad 1+z_{BH}=\left(1-\frac{r_{gE}r}{r^2+a^2}\right)^{-1/2}. \qquad (43)$$

In Fig. 10 corresponding plots the depending of $1+z$ on a are presented.

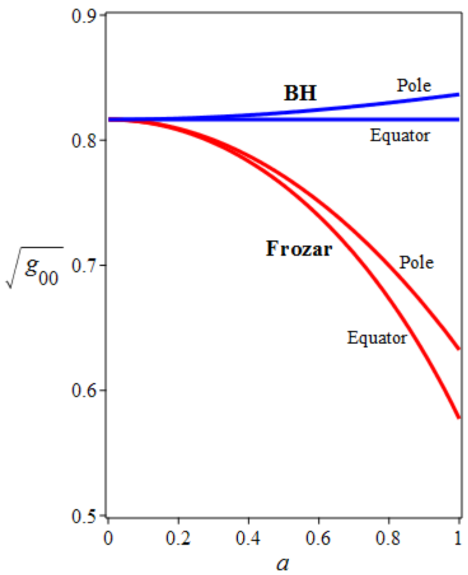

Fig. 9. Dependence on a of the time dilation factor $g_{00}^{1/2}(r,\theta)$ at $r=3r_{gP}$.

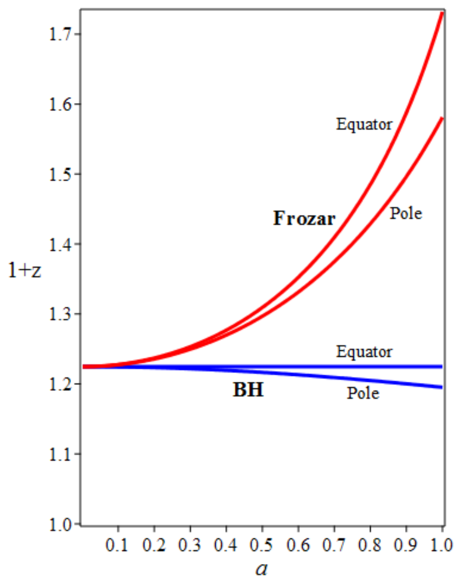

Fig. 10. Dependence on a of the redshift factor $1+z=g_{00}^{-1/2}(r,\theta)$ at $r=3r_{gP}$.

As in the case of a charge, in the case of a frozar, an increase in a reduces $g_{00}^{1/2}(r,\theta)$, as can be seen from (39), (41), (42), which is natural, since an increase in the rotational energy of the source at the same mass of matter enhances gravity outside it, and therefore increases time dilation and redshifts. However, in the BH theory with the condition $r_{gE}=const$, the opposite was claimed, that growth of a increases the factor $g_{00}^{1/2}(r,\theta)$ in (40) and (43), weakening gravity and reducing time dilation and redshifts.

3.3. Radii of orbits of photons and massive particles

The equations of motion and integrals of motion in the standard Kerr metric (22) with a dependent parameter $r_{gE}(a)$ are well known, and expressions for the radii of characteristic orbits are given in [9,14]. To obtain the corresponding expressions for the new form of the Kerr metric with independent parameters (31) it suffices to make the substitution (27) in all expressions for the observable effects. For this reason, we present only the results of such a replacement and the plots of the resulting dependencies on a.

Introducing the notation $a_* \equiv a / r_{gP}$, we write expression (27) for r_{gE} in the form:

$$r_{gE} = r_{gP}(1+a_*^2). \tag{44}$$

This gravitational radius at the equator grows as a^2 (Figs. 11a,12a).

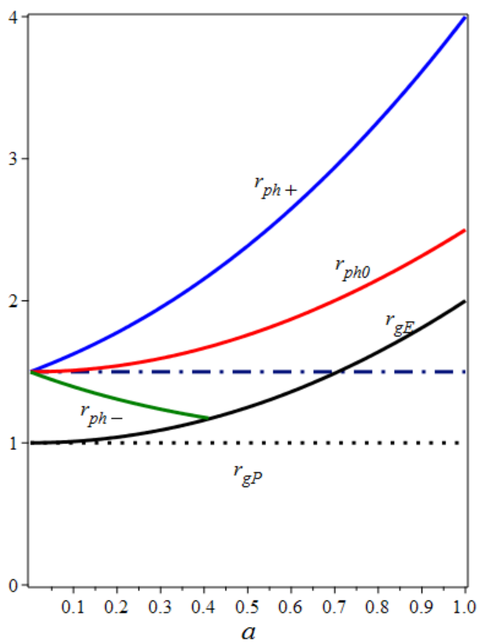

Fig. 11a. Radii of photon orbits in two directions of rotation $r_{ph\pm}$ and their average r_{ph0} for frozar in the new form of the Kerr metric.

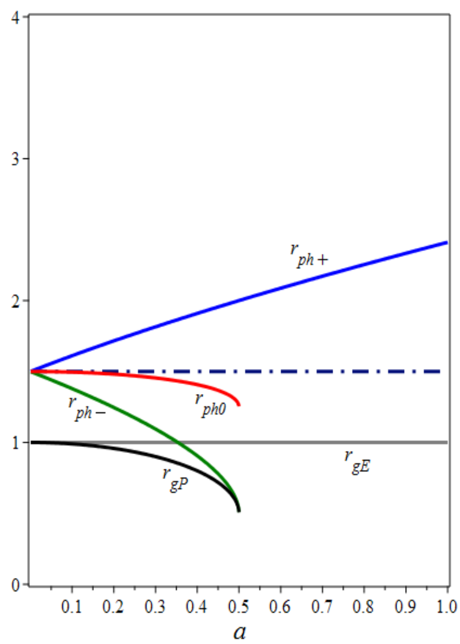

Fig. 11b. Radii of photon orbits in two directions of rotation $r_{ph\pm}$ and their average r_{ph0} in the standard Kerr metric for BHs.

The radii of the photon orbit $r_{ph\pm}$ in two directions of rotation on the orbit, and the average of these radii r_{ph0} (where the dragging effect is almost compensated) are (Fig. 11a):

$$r_{ph\mp} = r_{gP}(1+a_*^2)\left\{1+\cos\left[\frac{2}{3}\arccos\left(\mp\frac{2a_*}{1+a_*^2}\right)\right]\right\}, \quad r_{ph0} = \frac{1}{2}(r_{ph+} + r_{ph-}). \tag{45}$$

At $a = r_{gP}/2$, $a_* = 1/2$, for the upper sign (co-rotation) we have $r_{ph-} \simeq 1.13 r_{gP}$, for the lower sign (counter-rotation) $r_{ph+} \simeq 2.39 r_{gP}$, and their average is $r_{ph0} \simeq 1.76 r_{gP}$. They are larger than in the BH theory (Fig. 11b): $r_{ph-} \simeq 0.5 r_{gP}$, $r_{ph+} \simeq 2 r_{gP}$ and $r_{ph0} \simeq 1.25 r_{gP}$.

The radii of marginally bound orbits $r_{mb\pm}$ and r_{mb0} are equal to (Fig. 12a):

$$r_{mb\mp} = r_{gP}(1+a_*^2)\left(1\mp\frac{2a_*}{1+a_*^2}+\sqrt{1\mp\frac{2a_*}{1+a_*^2}}\right), \quad r_{mb0} = \frac{1}{2}(r_{mb-}+r_{mb+}). \tag{46}$$

At $a = r_{gP}/2$, $a_* = 1/2$, in the case of co-rotation $r_{ph-} = r_{gP}(3+\sqrt{5})/4 \simeq 1.31 r_{gP}$, and for counter-rotation $r_{ph+} = r_{gP}(7+3\sqrt{5})/4 \simeq 3.43 r_{gP}$, and $r_{mb0} = 2.37 r_{gP}$. These values are greater than predicted for BHs: $r_{ph-} \simeq 0.5 r_{gP}$, $r_{ph+} \simeq 2.91 r_{gP}$ and $r_{mb0} = 1.71 r_{gP}$ (Fig. 12b).

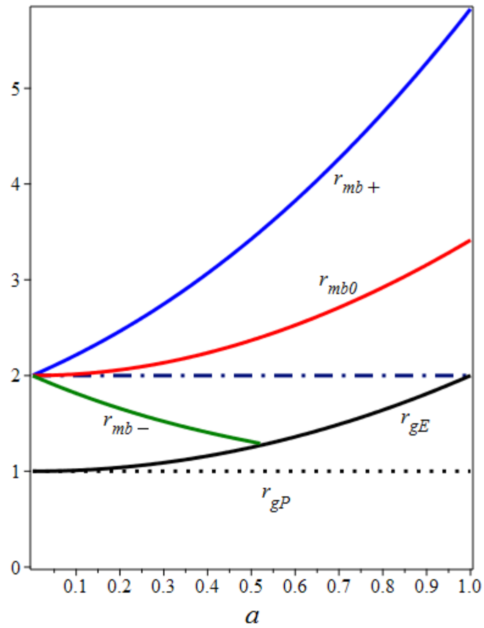

Fig. 12a. The radii of the marginally bound orbits $r_{mb\pm}$ in two directions of rotation on the orbit and their average r_{mb0} for frozar in the new form of the Kerr metric.

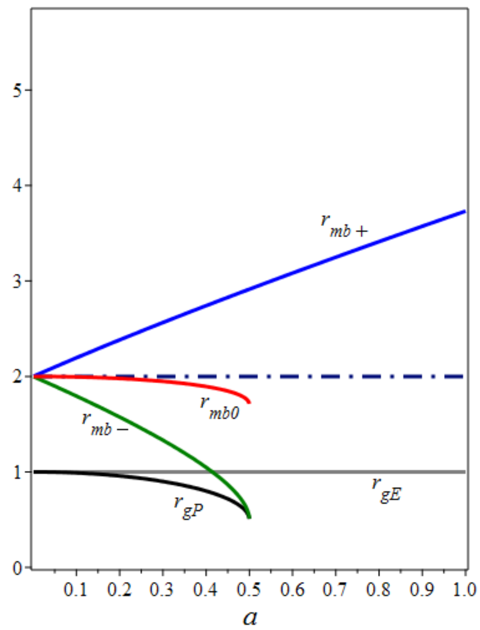

Fig. 12b. The radii of the marginally bound orbits $r_{mb\pm}$ in two directions of rotation on the orbit and their average r_{mb0} for BH in the stangard Kerr metric.

The radii of the innermost stable circular orbits $r_{ISCO\pm}$ are given by (Fig. 13a):

$$r_{ISCO\mp} = r_{gP}(1+a_*^2)\left\{\frac{3}{2}+Z_2\mp\left[\left(\frac{3}{2}-Z_1\right)\left(\frac{3}{2}+Z_1+2Z_2\right)\right]^{1/2}\right\}, \tag{47}$$

$$r_{ISCO0} = \frac{1}{2}(r_{ISCO-}+r_{ISCO+}), \tag{48}$$

$$Z_1 = \frac{1}{2}\{1+(1-b^2)^{1/3}[(1+b)^{1/3}+(1-b)^{1/3}]\}, \quad Z_2 = (Z_1^2+3b^2/4)^{1/2}, \quad b = \frac{2a_*}{1+a_*^2}$$

At $a = r_{gP}/2$, $a_* = 1/2$, we have $r_{ISCO-} \simeq 2.25 r_{gP}$ (co-rotation), $r_{ISCO+} \simeq 5.99 r_{gP}$ (counter-rotation) and their mean $r_{ISCO0} \simeq 4.12 r_{gP}$. These values are greater than in the BH theory (Fig. 13b): $r_{ISCO-} \simeq 0.5 r_{gP}$, $r_{ISCO+} \simeq 4.5 r_{gP}$ and $r_{ISCO0} \simeq 2.5 r_{gP}$.

3.4. The shadow of a rotating collapsar

From the plots of the previous section, it is clear that in the new form of the Kerr metric (31), the growth of a, increasing gravity, leads to an increase in the area of the collapsar's shadow, while in the previous predictions based on the standard form of the Kerr metric, the shadow decreased [9,17,18].

This can be seen in the example of the limiting case $a = r_{gE}/2$ ($a = \bar{M}$ in "geometric units"), where there is an explicit expression for the shadow contour for a distant observer on the equatorial plane. The projection of the shadow onto a plane perpendicular to the line between the observer and the center of the source is given by the formula (see Appendix):

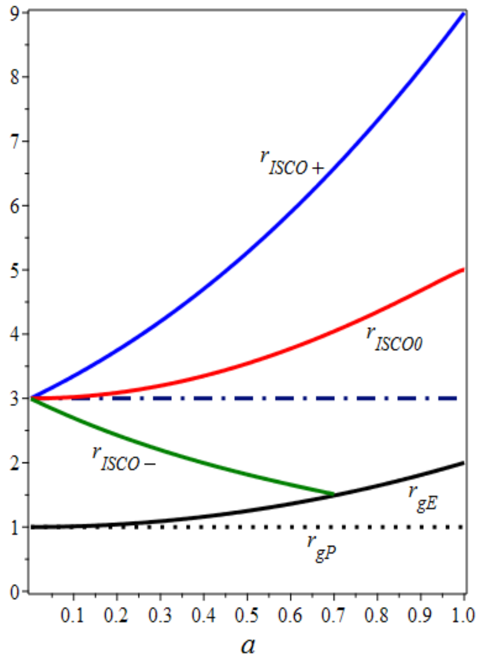

Fig. 13a. The radii of the lowest stable particle orbits $r_{ISCO\pm}$ and their mean r_{ISCO0} for frozar in the new form of the Kerr metric.

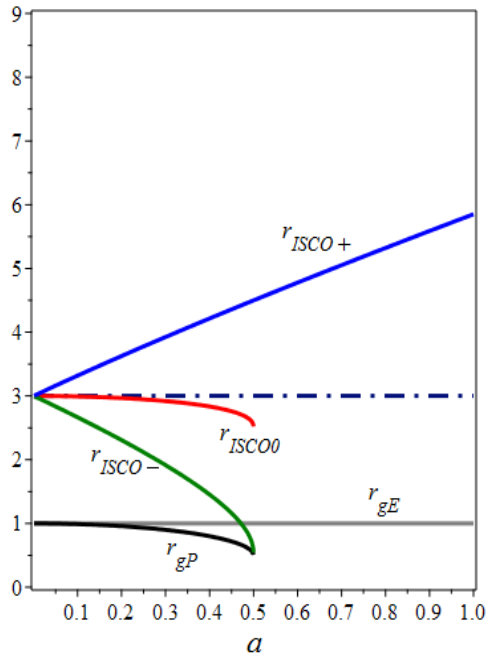

Fig. 13b. The radii of the lowest stable particle orbits $r_{ISCO\pm}$ and their mean r_{ISCO0} in the standard Kerr metric for BHs.

$$y(x) = \pm r_{gE}\frac{\tilde{r}}{2}\sqrt{\frac{1+3\tilde{r}^2-4x^2/r_{gE}^2}{\tilde{r}^2-1}}, \tag{49}$$

$$\tilde{r}(x) = 1+\sqrt{2(1+x/r_{gE})}, \tag{50}$$

where the axis y is directed along the rotation axis of the source, and the axis x lies on the equatorial plane. Taking into account the real dependence of r_{gE} on a according to (27) in this case gives $r_{gE} = 5r_{gP}/4$ and the shadow contour formula (49) takes the form:

$$y(x) = \pm r_{gP}\frac{5\tilde{r}}{8}\sqrt{\frac{1+3\tilde{r}^2-64x^2/25r_{gP}^2}{\tilde{r}^2-1}}, \tag{51}$$

$$\tilde{r}(x) = 1+\sqrt{2(1+4x/5r_{gP})}. \tag{52}$$

The plots for (49) and (51) are shown in Fig. 14.

The expressions in the general case, described in [18], are presented in the Appendix by taking into account (27). Plots of the shadow are shown in Fig. 15.

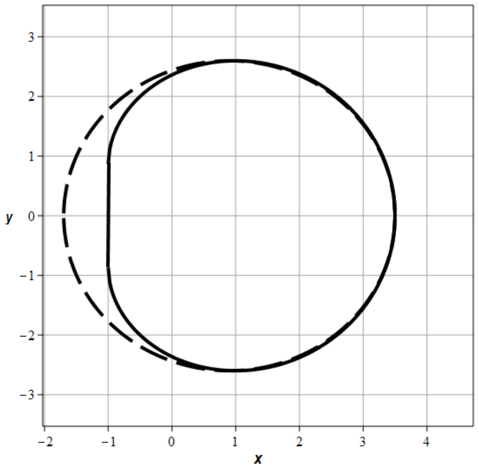

Fig. 14a. BH shadow contour at $a = r_{gE}/2$. Dashed line for $a = 0$ (shifted for comparison).

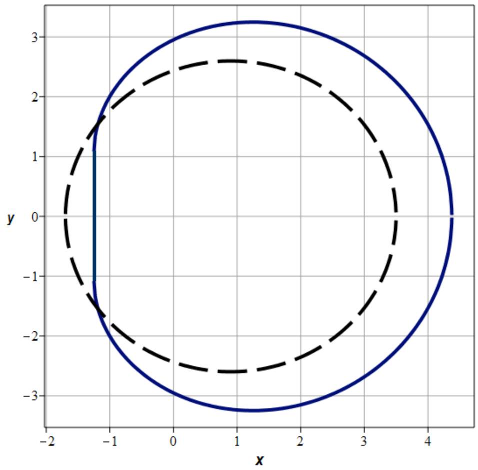

Fig. 14b. Frozar shadow at $a = r_{gP}/2$. Dashed line for $a = 0$ (shifted as in Fig 14a for comparison).

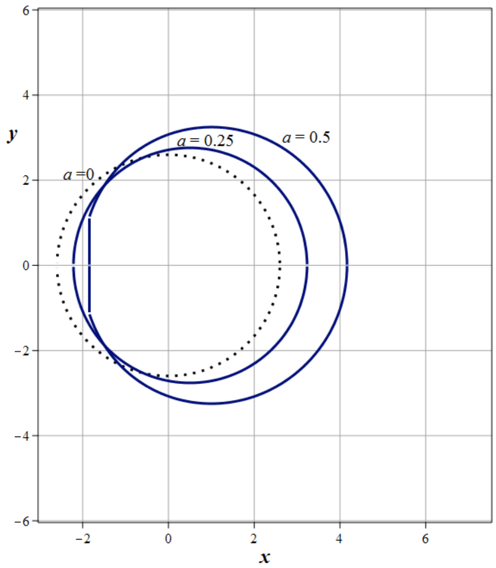

Fig. 15a. Shadow of frozar at $a = (0.25;\ 0.5) r_{gP}$.

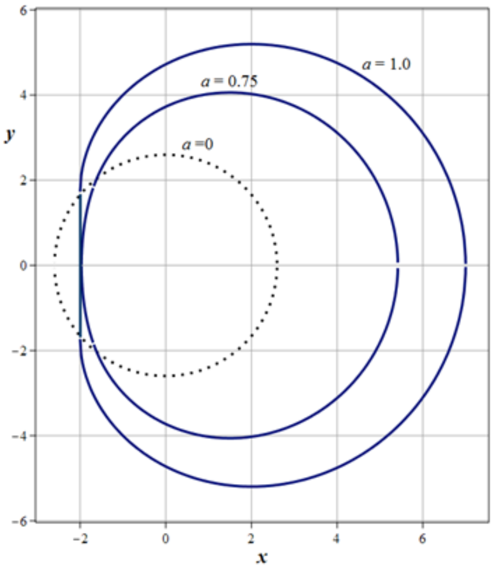

Fig. 15b. Shadow of frozar at $a = (0.75;\ 1.0) r_{gP}$.

4. Collapsar with angular momentum and charge on the surface

4.1. Modified Kerr-Newman metric with independent parameters

The standard KN metric [8,9] around a compact source with the rotation parameter a and the charge Q (Fig. 16) follows from the standard Kerr metric (22) at the replacement $r_{gE} r \to r_{gEQ} r - Q^2$, where r_{gEQ} turns to the gravitational radius at equator r_{gE} in the limit $Q = 0$. The line element with such a metric takes the form:

$$ds^2 = \left(1 - \frac{r_{gEQ} r - Q^2}{\rho^2}\right) c^2 dt^2 - \frac{\rho^2}{\Delta_Q} dr^2 - \rho^2 d\theta^2 + \frac{2a(r_{gEQ} r - Q^2)}{\rho^2} \sin^2\theta \, c dt d\varphi - \\ - \left(r^2 + a^2 + \frac{a^2 (r_{gEQ} r - Q^2)}{\rho^2} \sin^2\theta\right) \sin^2\theta \, d\varphi^2, \tag{53}$$

$$\Delta_Q(r) = r^2 - r_{gEQ} r + a^2 + Q^2. \tag{54}$$

The collapse of a star with angular momentum and a charge on the surface leads to the formation of a star with a frozen structure (frozar), whose spheroidal surface asymptotically tends to the gravitational radius $r_{g\theta Q}$ (Fig. 16b).

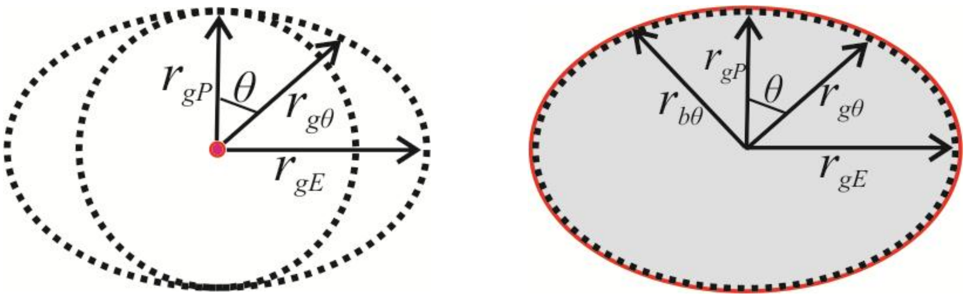

Fig. 16a. The structure of a rotating charged BH. All radii are "areal radii".

Fig. 16b. Structure of a frozar with angular momentum and the charge at the surface $r_{b\theta}$.

As in the case of a neutral frozar with angular momentum, the gravitational radius at the pole $r_{g\theta}\big|_{\theta=0} = r_{gP}$ follows from the condition:

$$g_{00}(r_{gP}, 0) = \frac{\Delta_Q(r_{gP})}{r_{gP}^2 + a^2} = 0, \qquad \Delta_Q(r_{gP}) = r_{gP}^2 - r_{gEQ} r_{gP} + a^2 + Q^2 = 0. \tag{55}$$

Dividing the last equality by r_{gP} we obtain the expression for r_{gEQ} in terms of r_{gP} [2]:

$$r_{gEQ} = r_{gP} + \frac{a^2 + Q^2}{r_{gP}}. \tag{56}$$

This allows us to write $\Delta_Q(r)$ in (54) through the independent r_{gP}:

$$\Delta_Q(r) = r^2 - \left(r_{gP} + \frac{a^2 + Q^2}{r_{gP}}\right) r + a^2 + Q^2 = r^2 \left(1 - \frac{r_{gP}}{r}\right)\left(1 - \frac{a^2 + Q^2}{r_{gP} r}\right). \tag{57}$$

Substituting this and (56) into (53), we obtain the line element at the pole:

$$ds^2 = \frac{r^2\Delta_Q}{\bar{\rho}^2}c^2dt^2 - \frac{\bar{\rho}^2}{r^2\Delta_Q}dr^2. \tag{58}$$

where $\bar{\rho}^2 = r^2 + a^2$. Here the role of r_{gP} as the gravitational radius at the pole is clear.

At inserting (56) into (53), the line element at the equator takes the form:

$$ds^2 = \frac{\Delta_Q - a^2}{r^2}c^2dt^2 - \frac{dr^2}{\Delta_Q} - \left(r^2 + a^2 + \frac{a^2K}{r}\right)d\varphi^2 + \frac{2aK}{r}cdtd\varphi, \tag{59}$$

$$K = r_{gP} + \frac{a^2 + Q^2(1 - r_{gP}/r)}{r_{gP}} \tag{60}$$

In contrast to (53), it is clearly seen here that an increase in a and Q, which does not affect on r_{gP}, leads to a decrease in g_{00}, and hence to enhancing the gravity of the source. The gravitational radius at the equator $r_{g\theta}\big|_{\theta=\pi/2} = r_{gE}$ we find from the condition:

$$g_{00}(r_{gP}, \pi/2) = \frac{\Delta_Q(r_{gE}) - a^2}{r_{gE}^2} = 0, \quad r_{gE}^2 - \left(r_{gP} + \frac{a^2 + Q^2}{r_{gP}}\right)r_{gE} + Q^2 = 0 \tag{61}$$

which gives:

$$r_{gE} = \frac{r_{gEQ}}{2} + \sqrt{\frac{r_{gEQ}^2}{4} - Q^2} = \frac{1}{2}\left(r_{gP} + \frac{a^2 + Q^2}{r_{gP}}\right) + \sqrt{\frac{1}{4}\left(r_{gP} + \frac{a^2 + Q^2}{r_{gP}}\right)^2 - Q^2}. \tag{62}$$

Thus, in the standard form of the KN metric (53), one of the three parameters included in it, r_{gEQ}, depends on the other two parameters a and Q, and to pass to independent parameters, it is necessary to express r_{gEQ} through r_{gP} according to (56). Substituting (56) into (53), taking into account (57) and (60), we arrive at a modified KN metric with three independent parameters a, Q and r_{gP}:

$$\begin{aligned} ds^2 = {} & \left(1 - \frac{rK}{\rho^2}\right)c^2dt^2 - \frac{\rho^2}{\Delta_Q}dr^2 - \rho^2 d\theta^2 + \frac{2a}{\rho^2}rK\sin^2\theta \cdot cdtd\varphi - \\ & - \left(r^2 + a^2 + \frac{a^2rK}{\rho^2}\sin^2\theta\right)\sin^2\theta\, d\varphi^2, \end{aligned} \tag{63}$$

The gravitational radius $r_{g\theta}$ we find from the condition $g_{00}(r_{g\theta}, \theta) = 0$, which gives [2]:

$$r_{g\theta}^2 - \left(r_{gP} + \frac{a^2 + Q^2}{r_{gP}}\right)r_{g\theta} + a^2\cos^2\theta + Q^2 = 0. \tag{64}$$

Solving this equation, we express $r_{g\theta}$ in terms of independent parameters:

$$r_{g\theta} = \frac{1}{2}\left(r_{gP} + \frac{a^2 + Q^2}{r_{gP}}\right) + \sqrt{\frac{1}{4}\left(r_{gP} + \frac{a^2 + Q^2}{r_{gP}}\right)^2 - a^2\cos^2\theta - Q^2}. \tag{65}$$

At the pole this gives r_{gP}, and at the equator it turns to r_{gE} from (62).

In the general case, $r_{g\theta}$ describes the surface of a frozar as an oblate spheroid (up to a small correction) where its charge is located. Due to centrifugal forces, the surface charge density at the equator is higher than at the pole, and this leads to a deformation of the electric field. The equipotential surfaces will be flattened at the poles and the observational effects of this fact, including the magnetic effects, will be discussed in more detail in the book [10].

At $r > r_{gP}$, the metric (63) is free of singularities, and it is clearly seen that an increase in a and Q reduces g_{00} and, therefore, enhances the gravity of the source due to the contribution of the rotational and the electric field energies. Therefore, the radii of orbits and shadows, redshifts in the field of such a source increase with increasing a and Q.

Previous predictions of BH theory for the dependence of observable effects on changes in a or Q, made at a constant parameter r_{gEQ}, should also be replaced by the new predictions with correctly taking into account (56).

4.2. Proper time dilation and redshifts

The dilation of the proper time interval $\Delta\tau = \Delta t\, g_{00}^{1/2}(r,\theta)$ between two events at a point (r,θ,φ) around the source with angular momentum and charge, according to (31), is given by the expressions for frozar and BH, respectively:

$$\Delta\tau_{froz} \simeq \Delta t\left(1-\frac{rK}{\rho^2}\right)^{1/2}. \tag{66}$$

$$\Delta\tau_{BH} \simeq \Delta t\left(1-\frac{r_{gEQ}r-Q^2}{\rho^2}\right)^{1/2}. \tag{67}$$

where K is given by (60). At the equator ($\theta=\pi/2$) we have:

$$\Delta\tau_{froz} \simeq \Delta t\left(1-\frac{r_{gP}}{r}-\frac{a^2+Q^2(1-r_{gP}/r)}{r_{gP}r}\right)^{1/2}, \tag{68}$$

$$\Delta\tau_{BH} \simeq \Delta t\left(1-\frac{r_{gEQ}}{r}+\frac{Q^2}{r^2}\right)^{1/2}, \tag{69}$$

and at the pole ($\theta=0$):

$$\Delta\tau_{froz} \simeq \frac{\Delta t}{(1+a^2/r^2)^{1/2}}\left(1-\frac{r_{gP}}{r}\right)^{1/2}\left(1-\frac{a^2+Q^2}{r_{gP}r}\right)^{1/2}, \tag{70}$$

$$\Delta\tau_{BH} \simeq \frac{\Delta t}{(1+a^2/r^2)^{1/2}}\left(1-\frac{r_{gEQ}}{r}+\frac{a^2+Q^2}{r^2}\right)^{1/2}. \tag{71}$$

The plots of dependence of $g_{00}^{1/2}(r,\theta)$ on a and Q are shown in Fig. 17.

Photons emitted at the point (r,θ,φ) near the frozar with a frequency ω in terms of t and received by a distant observer are compared with the frequency ω_0 of local photons (emitted near the observer), which gives $\omega < \omega_0$. The redshift factors $1+z = \omega_0 / \omega = g_{00}^{-1/2}(r,\theta)$, according to (68)-(70), are given by the expressions:

$$1+z_{froz} \simeq \left(1-\frac{rK}{\rho^2}\right)^{-1/2}. \tag{72}$$

$$1+z_{BH} \simeq \left(1-\frac{r_{gEQ}r-Q^2}{\rho^2}\right)^{-1/2}. \tag{73}$$

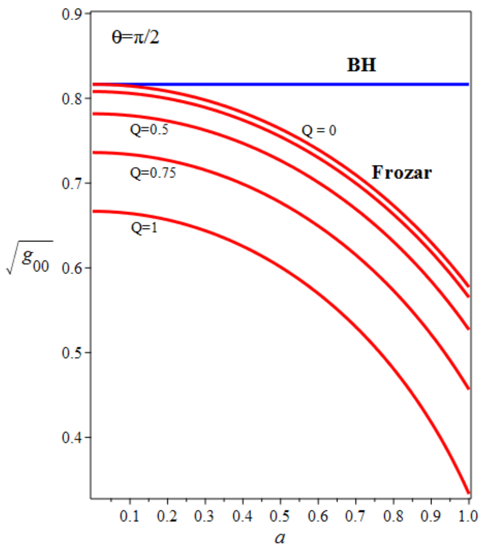

Fig. 17a. Dependence of the time dilation factor $g_{00}^{1/2}(r)$ on a in (68) for $r = 3r_g$ and $\theta = \pi/2$ for frozar with $r_b \simeq r_g$ and BH (69).

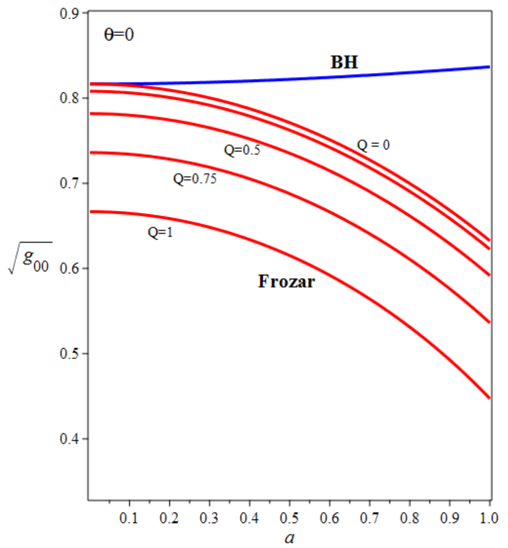

Fig. 17a. Dependence of the time dilation factor $g_{00}^{1/2}(r)$ on a in (70) for $r = 3r_g$ and $\theta = 0$ for frozar with $r_b \simeq r_g$ and BH (71).

At the equator $\theta = \pi / 2$ we have:

$$1+z_{froz} \simeq \Delta t\left(1-\frac{r_{gP}}{r}-\frac{a^2+Q^2(1-r_{gP}/r)}{r_{gP}r}\right)^{1/2}, \tag{74}$$

$$1+z_{BH} \simeq \Delta t\left(1-\frac{r_{gEQ}}{r}+\frac{Q^2}{r^2}\right)^{1/2}, \tag{75}$$

and at the pole $\theta = 0$:

$$1+z_{froz} \simeq \left(1+\frac{a^2}{r^2}\right)^{1/2}\left(1-\frac{r_{gP}}{r}\right)^{-1/2}\left(1-\frac{a^2+Q^2}{r_{gP}r}\right)^{-1/2}, \tag{76}$$

$$1+z_{BH} \simeq \left(1+\frac{a^2}{r^2}\right)^{1/2}\left(1-\frac{r_{gEQ}}{r}+\frac{a^2+Q^2}{r^2}\right)^{-1/2}. \tag{77}$$

Fig. 18 shows the corresponding plots of the dependence $1+z$ on a and Q.

Thus, an increase in a and/or Q in the case of frozar reduces $g_{00}^{1/2}(r,\theta)$, i.e., increases the gravity of the source, increasing the degree of the proper time dilation and the magnitude of redshifts. In the BH theory with the condition $r_{gEQ} = const$, the result is opposite - the growth a and/or Q increases $g_{00}^{1/2}(r,\theta)$, weakening the gravity of the source, and therefore reduces the degree of dilation of proper time and the value of redshifts.

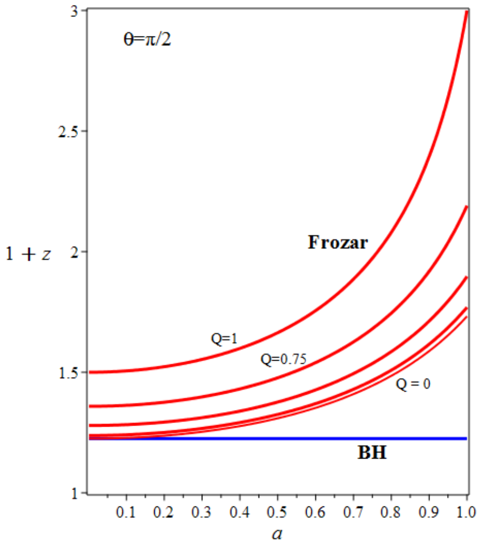

Fig. 18a. Dependence on a of the redshift $1+z = g_{00}^{-1/2}(r)$ at $r = 3r_g$ and $\theta = \pi/2$ for frozar (74) and BH (75).

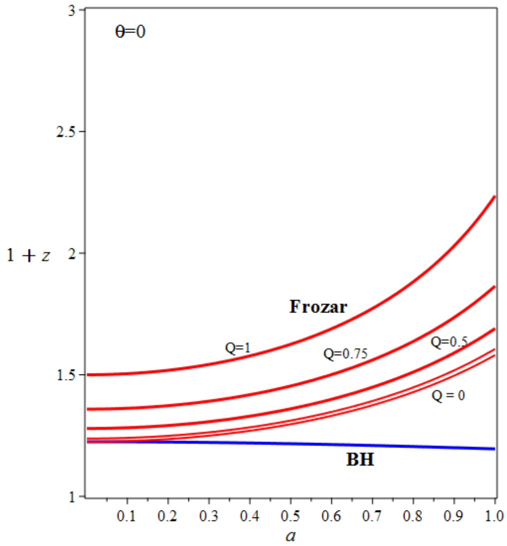

Fig. 18b. Dependence on a of the redshift $1+z = g_{00}^{-1/2}(r)$ at $r = 3r_g$ and $\theta = 0$ for frozar (76) and BH (77).

5. Conclusion

The metric outside a charged dust ball in the rest frame of its center is static and follows from Einstein's equations on hypersurfaces of simultaneity $t = const$. It was obtained earlier [11,12] under the assumption that the charge is distributed over the entire volume of the ball. However, firstly, the mass of the ball depends on the charge and the metric includes a parameter depending on another parameter, and secondly, in a real ball the charge lies on the surface.

In connection with these complications of the previous model of a ball with a volume charge, in the article [1] a simpler and more realistic model of a charged ball with a charge on the surface of radius r_b was considered. In this model, the mass M of the matter and its gravitational radius $r_g = 2GM/c^2$ do not depend on the charge Q. In the resulting metric with independent parameters r_b, r_g and Q the contribution of the electric field energy has the same sign as of the matter and therefore does not weaken, but strengthens gravity around the ball. As a result, the effects of gravity also increase, in particular, redshifts, radii of orbits and shadow (when r_b less than the radius of the shadow) will increase with growth of Q.

In Einstein's theory of gravity, the collapse of a dust ball, according to the Oppenheimer-Snyder solution [15] in terms of t, leads to the formation of a frozar, a star with a gravitationally frozen structure and with a surface near the gravitational radius of matter $r_b \to r_g$ [10,16]. It was shown in [1] that the metric for a charged frozar follows from the charged ball metric at $r_b \to r_g$. In this case, only two of the three parameters of the ball's metric in the frozar metric will remain two, r_g and Q. The observable consequences of the frozar metric are the same as for the ball, but with $r_b \simeq r_g$.

In [2], the method developed in [1] for reducing the metric to independent parameters was also applied to sources with angular momentum. The standard form of the metric outside a rotating source, both neutral (Kerr) and charged (KN), includes three parameters and one of them, the gravitational radius at the equator r_{gE} and r_{gEQ} depends on the other two, a and Q. In [2], these metrics were reduced to a form with independent parameters, in which r_{gE} and r_{gEQ} was replaced by the gravitational radius of the neutral non-rotating matter r_{gP}, independent of a and Q.

This made it possible to eliminate the previous non-physical predictions of the BH theory, that an increase in the rotation parameter a and/or the charge Q weakens gravity around the source, with a prediction of a weakening of the physical effects of gravity [9,14,17]. Instead, frozar theory, from which metrics with independent parameters follow naturally, predicts the opposite, that an increase in a and/or Q, by adding positive rotational and/or electric field energy, enhances gravity and increases the magnitude of its effects.

In this article, a brief review of the results of articles [1,2] was given and the consequences for some of the observable effects, in particular, time dilation, redshifts and shadows, were given. A more detailed study of the consequences of metrics with independent parameters and their further applications will be presented in the book [10].

Appendix. The shadow of a rotating collapsar

In the Kerr metric, the light-like equations of geodesics are separable and their solution is simplified by the presence of four constants of motion – the rest mass of a photon (equal to zero), energy E, angular momentum L, and the Carter constant Q [9,17]. The shadow edge coordinates (x, y) on the image plane, seen by a distant observer on the equatorial plane, are related to these constants as [18]:

$$x \simeq -\frac{L}{E}, \quad y = \pm\frac{\sqrt{Q}}{E}. \tag{78}$$

For a spherical orbit of a photon of radius r, they satisfy the relations:

$$x = \frac{r^3 + a^2 r + (a^2 - 3r^2) r_{gEQ}/2}{a(r - r_{gEQ}/2)}, \tag{79}$$

$$y = \pm\sqrt{\frac{3r^2 + a^2 - x^2}{1 - a^2/r^2}}. \tag{80}$$

Relation (79) is an equation for r:

$$r^3 - (3r_{gEQ}/2) r^2 + a(a - x) r + 3a(a + x) r_{gEQ}/2 = 0, \tag{81}$$

which can be solved by Vieta's trigonometric method. Introducing the notation

$$A(x) \equiv 1 - \frac{4a(a - x)}{3r_{gEQ}^2}, \quad B(x) \equiv \frac{2}{|A(x)|^{3/2}}\left(1 - \frac{4a^2}{r_{gEQ}^2}\right), \tag{82}$$

the solution can be written as $r(x) = \tilde{r}(x) r_{gEQ}/2$ [18], where:

$$\tilde{r}(x) = 1 + 2\sqrt{A}\cos\left(\frac{1}{3}\arccos B\right), \qquad A > 0,\ B \le 1, \tag{83}$$

$$\tilde{r}(x) = 1 + 2\sqrt{A}\cosh\left(\frac{1}{3}\ln\left(\sqrt{B^2 - 1} + B\right)\right), \qquad A \ge 0,\ B > 1, \tag{84}$$

$$\tilde{r}(x) = 1 - 2\sqrt{|A|}\sinh\left(\frac{1}{3}\ln\left(\sqrt{B^2 + 1} - B\right)\right), \qquad A < 0. \tag{85}$$

To obtain the edge of the shadow for given x, we calculate $r(x)$ from (83)-(85), then express r_{gEQ} through r_{gP} as in (56) and, substituting the result into (80), find $y(x)$.

References

1. Zakir Z. (2022) *Quant. and Grav. Phys*., **3**:016-7694.
2. Zakir Z. (2022) *Quant. and Grav. Phys*., **3**:017-7694.
3. Reissner H. (1916) *Ann. d. Phys*., **50**, 106.
4. Weyl H. (1917) *Ann. Phys*., **359**(18), 117.
5. Nordström G. (1918) *Proc. Kon. Ned. Akad. Wet*., **20**, 1238.
6. Kerr R. (1963) *Phys. Rev. Lett*., **5**, 1.
7. Boyer R., Lindquist R. (1967) *J. Math. Phys*. **8**, 265.
8. Newman E., Couch E., Chinnaparet K. et al (1965) *J. Math. Phys.* **6**, 918.
9. Bambi C. (2017) *Black Holes: A Lab. for Testing Strong Gravity*. Springer.
10. Zakir Z. (2022) *Theory of Frozars. Relativistic Collapse of Stars*, CTPA, T.
11. Bonnor W. (1960) *Z. Phys*., **160**, 59;
12. Florides P. (1960) *PhD Thesis*, *U. London*; (1962) *Math. Proc. Cambr. Phil. Soc*. **58**(1) 110; (1977) *Nuov. Cim*., **A42**(3), 343.
13. Christodoulou D., Ruffini R. (1971) *Phys. Rev*., **D4**, 3552.
14. Pugliese D., Quevedo H., Ruffini R. (2011) *Phys. Rev*. **D83**(2), 024021.
15. Oppenheimer R., Snyder H. (1939) *Phys. Rev*. **56**(1), 455.
16. Zakir Z. (2018) *Astr. & Space Sci*. **363**: 30; (2020) *Quant. & Grav. Phys*. **1**:006-7132; **1**:007-7133.
17. Bardeen J., Press W., Teukolsky S. (1972) *Astrophys. J.* **178**, 347.
18. Cunha P. V., Herdeiro C. A. (2018) *Gen. Rel. & Grav*., **50**(4), 1.